Combined PD-L1 and TIM-3 blockade improves the expansion of fit human CD8+ antigen-specific T cells for adoptive immunotherapy

Shirin Lak[1], Valérie Janelle[1], Anissa Djedid[2], Gabrielle Boudreau[1], Ann Brasey[1,3], Véronique Lisi[2], Cédric Carli[1], Lambert Busque[1,3,4,5], Vincent-Philippe Lavallée[2,6,7], Jean-Sébastien Delisle[1,4,5]

[1] Centre de recherche de l'Hôpital Maisonneuve-Rosemont, Montréal, Qc, Canada
[2] Centre de recherche du CHU Sainte-Justine, Montréal, Qc, Canada
[3] Biomarker Unit, Centre C3i, Montréal, Qc, Canada
[4] Department of Medicine, Université de Montréal, Montréal, Qc, Canada
[5] Hematology-Oncology and Cell therapy Division, Hôpital Maisonneuve-Rosemont, Montréal, Qc, Canada
[6] Department of Pediatrics, Université de Montréal, Montréal, Qc, Canada
[7] Hematology-Oncology Division, CHU Sainte-Justine CHU Sainte-Justine

Correspondence to:

Jean-Sébastien Delisle MD, FRCPC, PhD
Centre de recherche de l'Hôpital Maisonneuve-Rosemont
5415, Boul de L'Assomption
Montréal, Qc H1T 2M4
Canada
js.delisle@umontreal.ca

Word count
Abstract: 343
Main text: 5081

Declarations

Ethics approval and consent to participate. Informed consent was obtained from all cell donors as detailed in the Method section.

Consent for publication. All authors have reviewed the final version and agreed with the submission. The corresponding author agrees to pay the publication charges.

Availability of data and material. As detailed in the Methods section, the genomic data have been deposited for public access and agree to share protocols. All materials used are commercially available.

Competing interest. The authors have no relevant conflict of interest to disclose.

Funding. This work was funded by the Leukemia/Lymphoma Society of Canada (grants #622735 and #430053) to JSD.

Authors' contribution. SL and JSD conceived the study. SL, VJ, AB, CC performed experiments. SL, VJ, AB, AD, GB, VL analyzed data. LB, VPL, JSD oversaw data analysis. SL, VJ and JSD wrote the manuscript. All authors reviewed the manuscript.

Acknowledgments. The authors are grateful to the volunteer blood donors and Héma-Québec for the leukocytes reduction chamber procurement and handling. We also acknowledge the valuable contribution of Martine Dupuis (flow cytometry and sorting) and the Genome Québec staff for the single-cell RNA-sequencing. SL and VJ are respectively former Cole Foundation and Fonds de recherche du Québec-Santé (FRQS) studentship awardees, JSD and VPL hold FRQS clinician-scientist career awards and JSD is a member of the ThéCell network and of the Canadian Donation and Transplant Research Program (CDTRP).

List of Abbreviations

ACT	Adoptive Cell Therapy
APC	Antigen Presenting Cell
CCR7	C-C chemokine receptor type 7
CD	Cluster of differentiation
CDR	Complementarity Determining Region
CTLA-4	Cytotoxic T-lymphocyte-associated protein 4
CTLs	Cytotoxic T-lymphocytes
CTV	Cell Trace Violet
CTY	Cell Trace Yellow
DC	Dendritic Cell
DMSO	Dimethylsulfoxide
EBV	Epstein-Barr virus
ELISPOT	Enzyme-linked mmune absorbent spot
FBS	Fetal Bovine Serum
FOXP3	Forkhead Box P3
Gal-9	Galectin-9
GM-CSF	Granulocyte-Macrophage Colony-Stimulating Factor
GrzB	GranzymeB
HLA	Human Leukocyte Antigen
HMGB1	High Mobility Group Protein B1
IFN	Interferon
Ig	Immunoglobulin
IL	Interleukin
KLRG1	Killer cell Lectin-like Receptor G1
LAG-3	Lymphocyte-Activation Gene 3
LRSC	Leuko Reduction System Chamber
mAB	Monoclonal Antibody
MHC	Major Histocompatibility Complex
NGS	Next-generation Sequencing
PBMC	Peripheral Blood Mononuclear Cell
PBS	Phosphate-buffered saline
PD-1	Programmed Cell Death-1
PD-L1	Programmed Death Ligand-1
PGE2	Prostaglandin E2
PHA	T-cell mitogen phytohemagglutinin
PMA	Phorbol 12-myristate 13-acetate

PS	Phosphatidyl Serin
RT	Room Temperature
SC-RNA	Singel Cell RNA
TAA	Tumor-Associated Antigen
TAP	Transporter associated with Antigen Processing
Tcm	Central Memory T cell
TCR	T-cell Receptor
Teff	Effector T cell
Tem	Effector Memory T cell
TGF-β	Transforming Growth Factor-β
TIM-3	T-cell Immunoglobulin and Mucin-domain Containing-3
TMB	3,3′,5,5′-Tetramethylbenzidine
TNF	Tumor Necrosis Factor
TSA	Tumor-Specific Antigen
Tscm	Stem-cell Like memory T cells
WT1	Wilms' tumor suppressor gene1

Abstract

Background. The stimulation and expansion of antigen-specific T cells *ex vivo* enables the targeting of a multitude of cancer antigens. However, clinical scale T-cell expansion from rare precursors requires repeated stimulations *ex vivo* leading to T-cell terminal effector differentiation and exhaustion that adversely impact therapeutic potential. We leveraged immune checkpoint blockade relevant to antigen-specific CD8+ human T cells to improve the expansion and function of T cells targeting clinically relevant antigens.

Methods. A clinically-compliant protocol relying on peptide-pulsed monocyte-derived dendritic cells and cytokines was used to expand antigen-specific $CD8^+$ targeting the oncogenic Epstein-Barr virus (EBV) and the tumor associated antigen (TAA) Wilms Tumor 1 (WT1) protein. The effects of antibody-mediated blockade of immune checkpoints applied to the cultures (T-cell expansion, phenotypes and function) were assessed at various time points. Genomic studies including single cell RNA (scRNA) sequencing and T-cell receptor sequencing was performed on EBV-specific T cells to inform about the impact of immune checkpoint blockade on the clonal distribution and gene expression of the expanded T cells.

Results. Several immune checkpoints were expressed early by *ex vivo* expanded antigen-specific $CD8^+$ T cells, including PD-1 and TIM-3 with co-expression matching evidence of T-cell dysfunction as the cultures progressed. The introduction of anti-PD-L1 (expressed by the dendritic cells) and anti-TIM-3 antibodies in combination (but not individually) to the culture led to markedly improved antigen-specific T-cell expansion based on cell counts, fluorescent multimer staining and functional tests. This was not associated with evidence of T-cell dysfunction when compared to T cells expanded without immune checkpoint blockade. Genomic studies largely confirmed these results, showing that double blockade does not impart particular transcriptional programs or patterns on TCR repertoires. However, our data indicate that combined blockade may nonetheless alter gene expression in a minority of clonotypes and have donor-specific impacts.

Conclusions. The manufacturing of antigen-specific $CD8^+$ T cells can be improved in terms of yield and functionality using blockade of TIM-3 and the PD-L1/PD-1 axis in combination. Overcoming the deleterious effects of multiple antigenic stimulations through PD-L1/TIM-3 blockade is a readily applicable approach for several adoptive-immunotherapy strategies.

Background

The vast majority of potentially actionable cancer antigens are major histocompatibility (MHC)-bound peptides. These include tumor-specific antigens (TSA) resulting from mutated proteins or aberrantly expressed regions of the genome, tumor associated antigens (TAA) that come from abnormally expressed self-proteins and finally, non-self peptides best described in the setting of virus-associated cancers or allogeneic stem cell transplantation[1 2]. While it has been possible to isolate TSA or TAA-specific T-cell receptors (TCR) and manufacture TCR-transgenic T cells for adoptive immunotherapy, this approach faces numerous technical hurdles and is currently available only for a minority of relevant cancer antigens[3]. Several effective adoptive immunotherapy strategies rely on the *ex vivo* expansion of native antigen-specific T cells, enabling the targeting of a vast array of antigens. However, the expansion of large numbers of antigen-specific T cells requires repeated antigen exposure (through co-culture with antigen-presenting cells – APC) and stimulatory cytokines, potentially leading to T-cell dysfunction (terminal effector differentiation and exhaustion) and poor performance following adoptive transfer[4-6].

Alternatively, the endogenous cancer-reactive T-cell repertoire can be mobilized through the systemic administration of antibodies that prevent signaling from inhibitory co-signaling receptors present on the surface of exhausted T cells[7 8]. Such "immune-checkpoint" blockade, targeting most commonly Cytotoxic T-lymphocyte-associated protein 4 (CTLA-4) and Programmed death-1 (PD-1) on T cells (or its corresponding primary ligand, Programmed death-ligand 1 - PD-L1), is now the cornerstone of therapeutic regimes against several types of neoplasia including advanced melanoma and lung cancer[9]. As dysfunctional cancer-reactive T cells often express multiple negative co-signaling molecules, a strategy has been to use combined approaches with the caveat that increased response may come with more immune-related toxicities[10]. *Ex vivo* expanded T cells express inhibitory receptors, and PD-L1/PD-L2 silenced antigen-presenting dendritic cells have been shown to improve the expansion and function of antigen-specific T cells *ex vivo*[11], thus providing a solid rationale to leverage immune checkpoint blockade to improve T-cell manufacturing for adoptive immunotherapy.

158 We show herein that the *ex vivo* expansion of CD8+ T cells specific for a viral antigen and a TAA is
159 enhanced by using combined PD-L1 and T-cell immunoglobulin and mucin-containing protein-3 (TIM-3)
160 blockade, while single blockade or either receptor fails to improve T-cell expansion. The generated antigen-
161 specific T cells did not show phenotypic and functional evidence of exhaustion or terminal effector
162 differentiation. This was corroborated with single-cell RNA (sc-RNA) and VD(J) sequencing, which revealed
163 that dual immune checkpoint blockade can impact T-cell gene expression in a donor and clonotype-
164 dependent fashion. Taken together, our results show that dual PD-L1/TIM-3 blockade during *ex vivo*
165 expansion can yield large quantities of fit human antigen-specific T cells for adoptive immunotherapy.

166

Methods

Donors and cellular procurement

Peripheral blood mononuclear cells (PBMCs) from HLA-A0201 expressing volunteer donors were isolated using Ficoll-Hypaque gradient (STEMCELL Technologies) from fresh whole blood (collected by venipuncture) or leukoreduction system chambers provided by Héma-Québec (LRSCs) as previously described[12 13]. All donors provided written informed consent, and all the experiments were approved by the Héma-Québec and Hôpital Maisonneuve-Rosemont Research Ethics Committees. Recovered PBMCs were either used immediately for experiments or resuspended in freezing media (90% fetal bovine serum and 10% dimethyl sulfoxide (DMSO)), transferred to Mr. Frosty containers (NALGENE^{TM} Cryo 1^{oC} freezing container), and stored in vapor-phase liquid nitrogen for future use.

Dendritic Cells (DCs) differentiation and antigen pulsing

Monocyte isolation and DC differentiation have been generated as previously described[4]. Briefly, monocytes were obtained using the adherence method whereby PBMCs were plated in adherent plastic plates (Sarstedt) in media (X-Vivo 15 medium (LONZA) supplemented with 5% human serum, 2 mM L-glutamine and 1mM Sodium Pyruvate (Gibco), 1000 U/ml (100 ng/ml) IL-4 and 800 U/ml (50ng/ml) GM-CSF (Both from STEMCELL technologies)) and incubated in a CO_2, 37°C incubator for 7 days. On day 4, media was replaced with fresh media supplemented with IL-4 and GM-CSF. On day 7, DCs were matured with maturation media containing 1000 U/ml (100 ng/ml) IL-4, 800 U/ml (50ng/ml) GM-CSF (Both from STEMCELL technologies), 10 ng/ml TNF-α (STEMCELL technologies), 1 µg/ml PGE2 (SIGMA), 10 ng/ml IL-1β (Feldan), 100 ng/ml IL-6 (Miltenyi Biotec) and loaded with desired peptide (1 µg/mL $LMP2_{426-434}$ (CLGGLLTMV) or 1 µg/mL $WT1_{37-45}$ (VLDFAPPGA), both from JPT Peptides. Lastly, DC media was supplemented with IFN-γ 1000U/ml (Feldan) for the last 24 hours of culture.

Ex Vivo expansion of antigen-specific T cells

Antigen-specific T cells were stimulated using a clinically compliant protocol as previously described ([4] and www.clinicaltrials.gov NCT03091933) from $15x10^6$ PBMCs and expanded through multiple weekly stimulations using irradiated (40 Gy) autologous, peptide-loaded monocyte-derived DCs at a 1:10

(DC:PBMC) in a G-Rex6® Well Plate vessel (Wilson Wolf Manufacturing, New Brighton, MN). Our complete T-lymphocyte culture (CTL) media (Advanced RPMI 1640, 10% human serum, 1X L-glutamine(Gibco)) was supplemented with the following cytokines; week 1: IL-21 (30 ng/mL) and IL-12 (10 ng/ mL) (Both from Feldan), week 2: IL-21, IL-2 (100 IU/mL), IL-7 (10 ng/mL) and IL-15 (5 ng/mL) (STEMCELL Technologies), subsequent weeks: IL-2, IL-7 and IL-15. Medium, including cytokines, was refreshed every 3 to 4 days, and specific T cell cultures were restimulated once every week with peptide-loaded monocyte-derived DCs (moDCs). Cell concentration was adjusted to 1:10 ratio each week. When indicated, cultures were supplemented with 20 µg/ml of anti-PD-L1 blocking mAb (BioXcell, 29E.2A3) or/and 10 µg/ml of anti-TIM3 blocking mAb (Biolegend, F38-2E2) with all media changes. Respective isotype antibodies, mouse IgG1 (BioXcell, MOPC-21) and InVivoMAb mouse IgG2b (BioXcell, MPC-11), were used at the same concentration where indicated. All cell cultures were performed in monitored incubators (37°C in 5% CO_2 and 5% air humidity). Cell viability and cell counts were assessed by the countess automated cell counter (Invitrogen) using trypan blue (Invitrogen) at a 1:1 ratio with the cellular suspension in cell counting chamber slides (Invitrogen-C10283).

Flow cytometry

The phenotype of mature DCs was assessed by cell surface expression of the following markers (antibody clone in parenthesis) CD80 (L307.4), CD86 (2331, FUN1), HLA-ABC (W6-32), CD11c (3.9), CD19 (HIB19) (all from BD Biosciences)), HLA-DR (LN3), and CD83 (HB15e) (both from Invitrogen). To detect antigen-specific $CD8^+$ T cells, up to 10^6 cells were suspended in phosphate-buffered saline (PBS) plus 2% fetal bovine serum (FBS) and stained with allophycocyanin (APC) labeled tetramers, MHC-Dextramers A*0201 (Immudex,), for 10 minutes in the dark at 4ºC. For additional cell surface markers and phenotyping, cells were stained with following antibodies: CD3 (SKY7), CD3 (UCHT1), CD8 (SK1), CD45RO (UCHL1), CD45RA (5H9), CCR7 (150503), LAG3 (T47.530), and CD4 (RPA-T4) all from BD Biosciences; CD62L (DREG-56), TIM3 (F38-2E2), PD-1 (EH12.2H7), KLRG1 (2F1/KLRG1), CD57 (HCD57), and PD-L1 (29E.2A3) from Biolegend and CD8 (RPA-T8) and CD244 (eBioDM244) from Invitrogen. Staining was performed at room temperature (RT) in the dark for 30 minutes. According to the manufacturer's instructions for intracellular detection of cytokines, cells were permeabilized, fixed and stained using the Foxp3 /

Transcription Factor Staining Buffer Set (eBioscience). Before the fixation step, up to 10^6 cells were stimulated to produce cytokines with the indicated peptide (0.5 µg/ml) (test condition) or PMA (50 ng/mL)-ionomycin (500 ng/mL) (Sigma-Aldrich) (positive control) and an irrelevant peptide (HLA-A0201 restricted but not used as a stimulator in the culture-negative control) for 4 h at 37°C. Cells are suspended in CTL media plus brefeldin A (Biolegend) to block the secretion of cytokines during the stimulation period. Cells were then harvested and stained for cell-surface markers, including CD3, CD4, and CD8 in 4 °C for 20 minutes. Next, fixed and permeabilized cells were stained with intracellular cytokine detection antibodies; IFN-γ (4S.B3), IL-2 (MQ1-17H12), and TNF-α (Mab11) all purchased from BD Biosciences) and Ki67 (ki-67) from Biolegend at RT for 20 minutes. Cell acquisition was performed on a Fortessa or LSR II flow cytometer (BD Biosciences), and data were analyzed with Flowlogic Software (inivai).

IFN-γ Enzyme-linked immune-spot (ELISpot)

ELISPOT assays were performed using Human IFN- ELISpot^{PLUS} kit (MABTECH), following the manufacturer's instruction. Briefly, pre-coated wells were washed 5 times with sterile PBS (200ul/well), then incubated with CTL media (100 ul/well) for 30 minutes in a 37 °C incubator with 5% CO_2. Cultured cells were added (5×10^4) to wells in duplicates and then stimulated with anti-CD3 mAb (positive control), irrelevant peptide (specificity control), and test peptide. After an 18-hour incubation the plates were washed with PBS (200ul/well) 5 times and incubated with detection antibody (7-B6-1-biotin, 1ug/ml, 100 ul/well) for 2 hrs at RT. Next, plates were washed with PBS (200ul/well) 5 times and incubated with streptavidin-HRP (100 ul/well) for 1 hr at room temperature. Lastly, plates were rewashed as above, and TMB substrate solution (100 ul/well) was added in darkness. Color development was stopped by washing extensively in deionized water after distinct spots emerged. Plates were dried, and the dots were counted using ELISpot reader (vSpot Reader Spectrum, AID).

Flow Cytometry-based Cytotoxicity assay

Flow cytometry-based cytotoxicity assay was performed using either Cell Trace Violet (CTV) or Cell Trace Yellow (CTY) (Invitrogen Life Technologies) labeled $LMP2_{426-434}$ pulsed as target cells as described before[14]. Briefly, target cells were prepared by stimulating autologous PBMCs with the T-cell mitogen phytohemagglutinin (PHA) (3×10^6 PBMCs/mL were incubated in T-cell media with 20 µg/mL PHA) for 3

247 days at 37 °C and 5% CO_2. Peptide pulsed (or not pulsed) target cells were co-cultured with LMP2-specific
248 T cells at various ratios for 4 hours in CTL plus 10% horse serum. Unpulsed target cells alone were used
249 as control. After incubation, cells were harvested, stained with LIVE/DEAD Fixable Aqua Dead Cell Stain
250 Kit, Life Technologies) according to manufacturers' instructions and viable target, cells were quantified by
251 flow cytometry using Flow Count Beads (Beckman Coulter). Cytotoxicity was calculated by comparing the
252 percentage of viable target cells in test conditions relative to control (100 - (Target cell alive/ Target cell
253 alone) × 100).

254 **Single-cell RNA sequencing and High-throughput TCR sequencing**

255 At indicated time points, T cells were sorted based on MHC-Dextramer and CD8 staining using FACS Aria
256 III (DB Biosciences). Post sorted purity of the sorted population was 94%. A fraction of the sorted antigen-
257 specific T cells was subjected to both VDJ and transcriptome sc-RNA sequencing at the Genome Quebec
258 facilities. Briefly, cells were counted and viability assessed using a hemocytometer and Trypan Blue. The
259 targeted cell recovery was set at 6000 cells and libraries were prepared using the kits Chromium Next GEM
260 Single Cell 5' Kit v2 and Chromium Single Cell Human TCR Amplification Kit (10x Genomics inc.), as per
261 the manufacturer's recommendations. Libraries were quantified using the Kapa Illumina GA with Revised
262 Primers-SYBR Fast Universal kit (Kapa Biosystems). Average size fragment was determined using a
263 LabChip GX (PerkinElmer) instrument. The 10X Single cells 5' libraries were sequenced on Illumina HiSeq
264 4000 PE28x98 while the 10X Single Cells VDJ (Human T) libraries were sequenced on Illumina HiSeq 4000
265 PE150. The Illumina control software was HCS HD 3.4.0.38, the real-time analysis program was RTA v.
266 2.7.7. bcl2fastq2 v2.20 was then used to demultiplex samples and generate fastq files. Reads were aligned
267 to GRCh38 genome assembly, gene expression matrices generated, and clonotype identification
268 performed using CellRanger v3.0.2. The resulting gene expression matrices were normalised by total UMI
269 counts per cell multiplied by the median UMI count per cell and natural-log transformed using Scanpy v1.4[15].
270 PhenoGraph[16] clustering was applied with k=20 and clusters with a median mitochondrial fraction greater
271 than 0.2 were filtered out. Clonotypes were defined by nucleotide sequences of alpha and beta chains. In
272 order to remove potential doublets, we restricted our analysis to cells in which exactly one alpha and one
273 beta chain were identified and retained only the most abundant clonotype for each alpha and beta chain.

The number of retained cells per sample is provided in Table S1. After filtering, individual count matrices were combined and normalized and log transformed together for downstream analyses.

For expression analysis, only abundant clonotypes in each donor were retained. Abundant clonotypes are defined as those identified in at least 10 cells in each condition and at a frequency over all cells of a donor greater than 0.01. Pathway expression is defined as the log2 of the sum of the normalized gene expression for every gene in the pathway. Genes associated with each pathway are listed in Table S2.

Significance of the changes in pathway expression between the control and double blockade conditions was assessed using a Mann-Whithney U test. The p-values returned for each pathway comparison were contrasted with those obtained when comparing the expression in the DDB and CTRL conditions to those in 1000 random gene sets with the same number of genes with identical expression distribution as the pathway of interest. For each random gene set, we computed the p-value of the comparison using the Mann-Whithney U test. We report the percentile ranking of the p-value in the true pathway compared to the p-values obtained from the random gene sets.

Bulk TCR repertoire profiling was performed from sorted multimer positive and negative $CD8^+$ T-cell RNA preserved in Trizol reagent (Invitrogen) using Next-Generation Sequencing (NGS) targeting the hypervariable complementarity-determining region 3 (CDR3) of the T cell receptor beta chain (TCRβ). TRIzolTM extracted RNA in combination with the PureLink RNA mini and microcolumn system (Thermo Fisher), quantified by UV spectrophotometry (Tecan), and QC was completed on Bioanalyzer chip (Agilent). TCRb amplicon libraries were prepared from 25 ng total RNA with the Oncomine™ TCR Beta-SR Assay for RNA (ThermoFisher Scientific). The TCRb libraries obtained were quantified on the ViiA 7 Real-Time PCR System with the Ion Library Taqman Quantitation kit (Thermo Fisher). NGS was completed on the Ion S5 semiconductor platform using an Ion 540 chip, prepared with the Ion Chef System (all from Thermo Fisher). TCRβ repertoire analysis was completed using the Ion Reporter Software (Thermo Fisher) and Immunarch package[17] analyses using R software. The data can be found in the Gene Expression Omnibus (GSE182537 and GSE181682).

Statistical Analysis

Statistical significance was analyzed were with the R software, version 4.0.4. Multiple group comparisons were performed using one-way ANOVA and Turkey post hoc test or the Kruskal-Wallis test with the Holm procedure to correct for multiple testing (if ANOVA requirements were not met). Paired Wilcoxon-Mann-Whitney tests were performed for two-group comparisons. p values of 0.05 or less were considered significant.

Results

Multiple stimulations are detrimental to antigen-specific T-cell expansion *ex vivo*

Antigen-specific T cells were stimulated using moDCs loaded with the peptide $LMP2_{426-434}$ (CLGGLLTMV), which is an HLA-A0201 restricted antigen from the oncogenic Epstein-Barr virus (EBV). Weekly *ex vivo* stimulations were performed in cytokine supplemented media, and antigen-specific expansion was assessed before each stimulation. While overall T-cell expansion progressed following each of four stimulations (albeit at limited pace after day 14 and two stimulations), the percentage and absolute number of antigen-specific CD8 T cells, as identified by fluorescent HLA-0201/ $LMP2_{426-434}$ multimer, stagnated despite additional stimulations (Figure 1A-C). Further, this halted growth was matched with a gradual change in phenotype. The predominance of central memory (Tcm) differentiation profile at day 14 evolved towards an effector memory (Tem) and effector (Teff) differentiation phenotype on days 21 and 28 (Figure 1D). These results were anticipated as serial T-cell stimulations have been associated with the development of effector T cells that gradually lose their capacity to expand and persist after adoptive transfer[6]. The expression of the inhibitory receptors related to T-cell exhaustion (PD-1, TIM-3, and to a lesser extent LAG3 and 2B4) was substantial on a significant fraction of antigen-specific T cells at day 14, with little modulation over time in culture (Figure 1E). However, the fraction of cells showing dual expression of PD-1 and TIM-3 increased with repeated stimulation (Figure 1F) in line with the development of CD8+ T-cell exhaustion[18-20]. Phenotyping of the moDCs revealed prevalent expression of corresponding PD-1 and TIM-3 ligands, (respectively PD-L1 and CEACAM-1/Galectin 9) (Figure 1G). These results confirm and extend previous data, suggesting that the early and persistent expression of PD-1 and TIM-3 by $CD8^+$ T cells, along with the expression of their ligands by stimulating DCs, may represent a significant hurdle for the expansion of antigen-specific T cells for immunotherapy[18 19].

Combination of PD-L1/PD-1 axis and TIM-3 blockade significantly increases antigen-specific $CD8^+$ T-cell expansion

In order to assess if immune checkpoint blockade during *ex vivo* expansion may improve antigen-specific T-cell yield, anti-PD-L1, anti-TIM-3, or both were added to the culture media at the beginning of culture and with all media changes. Cell counts at day 14, and even more strikingly at day 21, revealed that the double

blockade condition significantly increased T-cell expansion relative to control (no checkpoint blockade) and the single blockade groups (Figure 2A). This translated into a marked increase in $LMP2_{426-434}$-specific T-cell yield in the dual blockade condition despite no gain (and in fact a decline at day 14) in the percentage of multimer positive $CD8^+$ T cells (Figure 2B-C). In contrast, the single blockade of PD-L1 or TIM-3 offered no advantage at any time point. The phenotypic assessment of $LMP2_{426-434}$-specific T cells revealed no statistically significant difference in the percentages of Tcm, Tem, and Teff and no difference in PD-1 or TIM-3 expression (Figure 2D-E). However, the percentage of T cells expressing the inhibitory receptors LAG3 and 2B4 was lower in the combined relative to the control condition. Hence, dual PD-L1 and TIM-3 blockade increased T-cell growth without conferring phenotypic changes associated with increased T-cell dysfunction.

It is known that TIM-3 has a dual function. TIM-3 is transiently upregulated at intermediate levels on activated T cells and confers activation signals[21]. However, in settings of chronic stimulation in the presence of its ligands, TIM-3 inhibits T-cell activation and behaves as a *bona fide* immune checkpoint. We, therefore, slightly modified our protocol to introduce TIM-3 blockade at day 7, a week after the first stimulation (hereafter designated as delayed double blockade-DDB), with the expectation that it would further improve antigen-specific T-cell yield. Compared to the dual blockade started on day 0, DDB slightly increased total T-cell expansion at day 21 and more convincingly following an additional antigenic stimulation (day 28) (Figure 3A). Moreover, the DDB approach increased the percentage of $LMP2_{426-434}$-specific T cells at all time points relative to the control condition (no blocking antibodies used), including at day 14 which was not the case when PD-L1 and TIM-3 blockade were both applied at day 0 (Figure 3B). Absolute antigen-specific counts were also increased in the DDB relative to the control condition (significant on days 21 and 28) (Figure 3C). Finally, DDB did not impact T-cell differentiation or exhaustion marker expression (Figure 3D-E). Independent cultures using isotype control antibodies confirmed the specific effects of anti-PD-L1 and anti-TIM-3 antibodies on the antigen-specific T-cell expansion (Supplementary Figure 1). We conclude that combined blockade of the PD-L1/PD-1 axis and TIM-3 can be incorporated in *ex vivo* cultures to increase antigen-specific $CD8^+$ T-cell yield for adoptive immunotherapy without altering T-cell phenotypes.

Double immune checkpoint blockade generates functional antigen-specific T cells

Dual PD-L1 and TIM-3 blockade increases antigen-specific CD8+ T-cell expansion in culture without altering T-cell phenotypes suggesting comparable functionality. Intracellular cytokine secretion measurements and ELISpot assays at day 28 confirmed that a higher proportion of T cells were reactive upon $LMP2_{426-434}$ peptide re-exposure in the DDB condition relative to control (no checkpoint inhibition) (Figure 4A-B). This was also generally the case when DDB was compared to double immune checkpoint blockade administered at day 0 (statistically significant in ELISPOT data at day 28). We thus pursued our functional assessments comparing DDB with the control condition. As further indication of increased functionality, a greater fraction of antigen-specific T cells expanded in the DDB condition relative to control expressed the proliferation marker Ki-67 and upon peptide re-exposure, more DDB exposed T cells displayed evidence of cytotoxic potential (surface CD107a and intracellular granzyme B expression) (Figure 4C-D). This was corroborated with cytotoxicity assays showing that T cells from the DDB condition were highly effective, especially at low effector:target ratios (Figure 4E-F). Importantly, in all our assays, combined PD-L1 and TIM-3 blockade did not lead to increased non-specific (off-target or spontaneous) cytokine release or cytotoxicity. Thus, dual immune checkpoint inhibition expands T-cell products with specific and augmented antigen reactivity.

PD-L1/TIM-3 blockade imparts no consistent gene expression signatures to expanded antigen-specific $CD8^+$ T cells

To gain more insight into the biological impacts of double immune checkpoint blockade on antigen-reactive T cells, we submitted sorted day 28 multimer-positive T cells from three donors to paired transcriptome and TCR alpha-beta single-cell RNA sequencing (scRNA-Seq). Gene expression was compared across donor, condition (no checkpoint blockade vs. DDB) and clonotypes. Global gene expression patterns across the three donors revealed strong donor-specific clustering (Figure 5A). The impact of DDB on gene expression for each donor antigen-specific T cells, was assessed using published human T-cell gene sets[22]. This enabled a detailed assessment of T-cell activation, proliferation, terminal differentiation, exhaustion and metabolism-associated gene expression as these processes are likely to be impacted by DDB. Overall, when every T cells from each condition were compared, no consistent change of gene expression signature

393 could be identified across all donors (Figure 5B). We next evaluated whether clonotype-specific signatures
394 could be identified. The sequencing of the VD(J) regions revealed that the $LMP2_{426-434}$ specific T cells were
395 highly oligoclonal in all donors and conditions (1-4 clones representing more than 80% of all cells – Figure
396 5C and Supplementary Table 3). Most dominant clonotypes were shared between experimental conditions
397 (albeit at different frequencies for Donor 2) and a few clonotypes were shared between donors
398 (Supplementary Table 3). We next analyzed the expression of several pathways in the abundant clonotypes
399 (defined as those identified in at least 10 cells and representing at least 1% of the repertoire in both the
400 DDB and control conditions from the same donor). Similar to comparisons involving all clonotypes, no
401 consistent pattern was found across donors when comparing the DDB versus control condition on a per
402 clonotype basis (Figure 5D). Interestingly, our data unveiled divergent gene expression patterns for one
403 clonotype (Clonotype 3) which was shared by Donor 1 and 2. Relative to its counterpart in the control
404 condition, Donor 1 Clonotype 3 in the DDB condition expressed higher levels of genes related to T-cell
405 exhaustion/differentiation and had a lowered expression of genes associated with T-cell proliferation. The
406 same clonotype in the DDB condition from Donor 2 had, on the contrary, an increased expression of the
407 genes associated with T-cell activation without any transcriptional changes related to T-cell dysfunction (T-
408 cell exhaustion, terminal differentiation, low proliferation). This suggests that donor rather than clonotype
409 related features may determine T-cell outcomes following DDB.
410
411 To assess whether clonotype-specific transcriptional signatures may impact their expansion and clonal
412 hierarchy within the cultures, we used bulk mRNA collected from sorted multimer negative and positive
413 CD8+ T cells at day 21 and 28 from the same donors. RNA of suitable quality was obtained for 23 out of a
414 potential of 24 samples (the multimer-positive fraction of the control condition from Donor 3 had to be
415 excluded) and subjected to complementary determining region 3 (CDR3) region sequencing of the T-cell
416 receptor-beta chain (TCRβ). Day 28 multimer-positive T-cell CDR3 sequencing matched very well paired
417 VDJ sequencing of single cells (Supplementary Figure 2), confirmed the oligoclonality of the multimer-
418 positive T cells at both day 21 and 28 and revealed that TCR repertoire diversity in the multimer-negative
419 T cells was not affected by DDB (Figure 6A). Further, the multimer positive and negative fractions had
420 limited overlap (Supplementary Figure 3), suggesting that sorting effectively separated most CD8+ antigen-

specific cells from the rest of the T cells in culture. Clonotype hierarchy among multimer-positive T cells at day 21 and day 28 showed no consistent pattern of evolution in DDB relative to the control condition (Figure 6B-C). However, the proportion of certain clonotypes in these fractions (both DDB and control) varied greatly (>20%) between day 21 and 28. This was notably the case for Clonotype 3 from Donor 1 in the DDB condition, which declined markedly from day 21 to day 28, whereas this clonotype's abundance did not change significantly between day 21 to 28 of DDB exposure in Donor 2 (Figure 6B). We wondered if the clonotypes with altered abundance between day 21 and day 28 in the same donor and condition displayed a specific transcriptional profile. In general, weak changes in transcriptional signatures were detected when comparing a given clonotype and experimental condition between day 28 and day 21. In the DDB condition, clonotype 3 of Donor 1, which showed a decreased abundance from day 21 to day 28, had a higher expression of genes related to T-cell activation, differentiation and exhaustion. This effect seems to be clonotype and donor specific but not condition specific since a similar behavior is seen in the control condition in clonotype 2 of Donor 3 (Figure 6D). Taken together these data show that DDB has limited impact on the clonal diversity of the expanded T cells overtime. The proportion of isolated clones can nonetheless fluctuate in line with their gene expression signatures at day 28. We noticed a weak trend of increased expression of genes related to exhaustion in clonotypes with decreased abundance at day 28 and a rise in the expression of genes related to proliferation in clonotypes with an increased abundance at day 28, irrespective of experimental conditions. Globally, these results suggest that DDB confers no consistent transcriptional features to expanded antigen-specific $CD8^+$ antigen-specific T cells but may alter activation/dysfunction, cell cycle and metabolic processes in a clonotypes and donor-dependent fashion.

The benefits of dual PD-L1 and TIM-3 blockade extend to TAA-specific T cells

The EBV-derived $LMP2_{426-434}$ antigen stimulates a memory T-cell repertoire in more than 90% of adults[23]. The *ex vivo* expansion of naïve T cells is generally considered more challenging for several reasons (size of the repertoire, amount of stimulation required, etc.). We, therefore, sought to determine the impact of dual PD-L1/TIM-3 blockade in the priming and expansion of naïve T cells. It was previously shown that CD8+ T cells specific against Wilm's tumor 1 (WT1) derived peptides, a clinically relevant tumor-associated antigen (TAA), are phenotypically naïve in healthy individuals[24] but can be expanded from a majority of

449 such donors[25 26]. Volunteer donor T cells were stimulated with an HLA-0201 restricted WT1 peptide ($WT1_{37-45}$) using the same stimulation/expansion conditions for $LMP2_{426-434}$ specific T cells. Figure 7A-C shows that
451 WT1-specific T cells expanded following a similar pattern as $LMP2_{426-434}$-specific T cells. The expansion,
452 percentages and number of antigen-specific cells as well as their cytokine secretion were improved in the
453 DDB condition relative to cultures without immune checkpoint blockade, again without altering T-cell
454 differentiation patterns or exhaustion marker expression (Figure 6D-G). We conclude that our results
455 obtained with $LMP2_{426-434}$ extend beyond virus-specific memory T-cell expansion and that double PD-
456 L1/TIM-3 immune checkpoint blockade can improve the expansion of functional TAA-specific $CD8^+$ T cells
457 from naïve repertoires.
458

Discussion

The stimulation and expansion of antigen-specific T cells for adoptive immunotherapy is an attractive strategy to target a wide variety of cancer antigens. However, T-cell expansion is limited by the expression of inhibitory receptors and the development of T-cell dysfunction. We confirmed and extended previous studies revealing that immune checkpoint receptors are expressed on repeatedly activated T cells and that their corresponding ligands can be present on antigen-presenting cells used *ex vivo*. Co-expression of PD-1 and TIM-3 has been used to describe highly exhausted $CD8^+$ T cells, and combined blockade of these receptors in murine models has previously been shown to improve tumor control relative to single blockade[18 19 27]. We show that antibody-mediated immune checkpoint blockade targeting PD-1 or TIM-3 alone is insufficient to improve $CD8^+$ T-cell expansion while the combination improves T-cell expansion and antigen-specific reactivity. These data confirm the synergistic potential of immune checkpoint blockade and the particular relevance of TIM-3 and PD-1 as inhibitory receptors in $CD8^+$ T cells[19]. The reasons for this synergistic effect might be due to the mobilization of different signaling intermediates by the two receptors. While PD-1 relies on the recruitment of SHP phosphatases to mediate its effects (as for several other negative co-stimulatory molecules), TIM-3 uses Bat3 and Fyn for its stimulatory and inhibitory effects, respectively. We reasoned that delaying TIM-3 blockade by one week after the start of the culture even in the presence of TIM-3 ligands on APC would be beneficial, given previous experimental evidence that TIM-3 provides activation signals following a first T-cell stimulation[28 29]. This contrasts with PD-1, which conveys inhibitory signals in both exhausted T cells and early after activation[30], justifying the use of anti-PD-L1 at culture initiation. We realize that several refinements may be required to fully leverage the potential agonistic/antagonistic effects of TIM-3 on T-cell activation and expansion and determine whether anti PD-L1/PD-1 blockade may also be improved by altering the timing of the inhibition. In addition, whether dual PD-L1/TIM-3 blockade improves T-cell expansion and function across multiple types of T-cell manufacturing protocols should be tested, just like further combinations with blockade of additional inhibitory receptors. Nonetheless, our work provides a new strategy for T-cell expansion and offers novel biological insights on the effects of PD-L1/PD-1 axis and TIM-3 blockade in human antigen-specific T-cell clonotypes submitted to multiple antigenic stimulations.

Our data support that sustained dual PD-L1/TIM-3 blockade through several rounds of antigenic stimulations provides ongoing benefits without exacerbating T-cell dysfunction or curbing expansion as inferred by previous studies of using inhibitory receptor gene deletion[31]. This was assessed through phenotyping, functional assays, and gene expression in single cells. Our results indicate that antigen-specific $CD8^+$ T cells expanded under combined TIM-3/PD-L1 blockade are functional as well as specific and that their clonal composition is generally stable in time and relative to their counterpart not exposed to immune checkpoint blockade. It has been reported that immune checkpoint blockade *in vivo* can shape the T-cell repertoire[32-34]. Thus, from a perspective of T-cell therapy, it was essential to define whether an intervention during *ex vivo* T-cell expansion alters the clonal identity of the cellular product. While we did not observe consistent effects of PD-L1/TIM-3 blockade on T-cell transcriptome or clonotype distribution, altered transcriptional profiles in a clonotype and donor-dependent manner nonetheless suggests that immune checkpoint blockade in adoptive T-cell therapy may require personalization.

Further work will be required to understand why some clonotypes may be more susceptible to differentiation/exhaustion following immune checkpoint blockade (previous activation/proliferation history, differentiation status at the beginning of checkpoint blockade, etc). Nevertheless, our data suggest that even after 28 days in culture, the antigen-specific T cells are highly functional, with a third expressing Tcm markers. This indicates that antigen-specific T cells generated in high numbers after dual immune checkpoint blockade could further expand after transfer and likely respond to further immune checkpoint blockade administered *in vivo*.

We conclude that dual PD-L1/TIM-3 blockade is a readily applicable strategy to improve the expansion of functional antigen-specific $CD8^+$ T cells expansion *ex vivo* for adoptive immunotherapy.

References

1. Janelle V, Rulleau C, Del Testa S, et al. T-Cell Immunotherapies Targeting Histocompatibility and Tumor Antigens in Hematological Malignancies. *Front Immunol* 2020;11:276. doi: 10.3389/fimmu.2020.00276
2. Chrusciel E, Urban-Wojciuk Z, Arcimowicz L, et al. Adoptive Cell Therapy-Harnessing Antigen-Specific T Cells to Target Solid Tumours. *Cancers (Basel)* 2020;12(3) doi: 10.3390/cancers12030683
3. Oppermans N, Kueberuwa G, Hawkins RE, et al. Transgenic T-cell receptor immunotherapy for cancer: building on clinical success. *Ther Adv Vaccines Immunother* 2020;8:2515135520933509. doi: 10.1177/2515135520933509
4. Janelle V, Carli C, Taillefer J, et al. Defining novel parameters for the optimal priming and expansion of minor histocompatibility antigen-specific T cells in culture. *Journal of translational medicine* 2015;13:123. doi: 10.1186/s12967-015-0495-z
5. Gattinoni L, Klebanoff CA, Restifo NP. Paths to stemness: building the ultimate antitumour T cell. *Nat Rev Cancer* 2012;12(10):671-84. doi: nrc3322 [pii]

10.1038/nrc3322 [published Online First: 2012/09/22]
6. Janelle V, Delisle JS. T-Cell Dysfunction as a Limitation of Adoptive Immunotherapy: Current Concepts and Mitigation Strategies. *Cancers (Basel)* 2021;13(4) doi: 10.3390/cancers13040598
7. Wei SC, Duffy CR, Allison JP. Fundamental Mechanisms of Immune Checkpoint Blockade Therapy. *Cancer Discov* 2018;8(9):1069-86. doi: 10.1158/2159-8290.CD-18-0367
8. Chamoto K, Hatae R, Honjo T. Current issues and perspectives in PD-1 blockade cancer immunotherapy. *Int J Clin Oncol* 2020 doi: 10.1007/s10147-019-01588-7
9. Vaddepally RK, Kharel P, Pandey R, et al. Review of Indications of FDA-Approved Immune Checkpoint Inhibitors per NCCN Guidelines with the Level of Evidence. *Cancers (Basel)* 2020;12(3) doi: 10.3390/cancers12030738 [published Online First: 2020/04/05]
10. Schnell A, Bod L, Madi A, et al. The yin and yang of co-inhibitory receptors: toward anti-tumor immunity without autoimmunity. *Cell Res* 2020;30(4):285-99. doi: 10.1038/s41422-020-0277-x
11. Hobo W, Maas F, Adisty N, et al. siRNA silencing of PD-L1 and PD-L2 on dendritic cells augments expansion and function of minor histocompatibility antigen-specific CD8+ T cells. *Blood* 2010;116(22):4501-11. doi: 10.1182/blood-2010-04-278739
12. Boudreau G, Carli C, Lamarche C, et al. Leukoreduction system chambers are a reliable cellular source for the manufacturing of T-cell therapeutics. *Transfusion* 2019;59(4):1300-11. doi: 10.1111/trf.15121
13. Orio J, Carli C, Janelle V, et al. Early exposure to interleukin-21 limits rapidly generated anti-Epstein-Barr virus T-cell line differentiation. *Cytotherapy* 2015;17(4):496-508. doi: 10.1016/j.jcyt.2014.12.009
14. Dahmani A, Janelle V, Carli C, et al. TGFbeta Programs Central Memory Differentiation in Ex Vivo-Stimulated Human T Cells. *Cancer Immunol Res* 2019;7(9):1426-39. doi: 10.1158/2326-6066.CIR-18-0691
15. Wolf FA, Angerer P, Theis FJ. SCANPY: large-scale single-cell gene expression data analysis. *Genome Biol* 2018;19(1):15. doi: 10.1186/s13059-017-1382-0
16. Levine JH, Simonds EF, Bendall SC, et al. Data-Driven Phenotypic Dissection of AML Reveals Progenitor-like Cells that Correlate with Prognosis. *Cell* 2015;162(1):184-97. doi: 10.1016/j.cell.2015.05.047
17. Nazarov VI, Pogorelyy MV, Komech EA, et al. tcR: an R package for T cell receptor repertoire advanced data analysis. *BMC Bioinformatics* 2015;16:175. doi: 10.1186/s12859-015-0613-1
18. Zhou Q, Munger ME, Veenstra RG, et al. Coexpression of Tim-3 and PD-1 identifies a CD8+ T-cell exhaustion phenotype in mice with disseminated acute myelogenous leukemia. *Blood* 2011;117(17):4501-10. doi: 10.1182/blood-2010-10-310425
19. Sakuishi K, Apetoh L, Sullivan JM, et al. Targeting Tim-3 and PD-1 pathways to reverse T cell exhaustion and restore anti-tumor immunity. *J Exp Med* 2010;207(10):2187-94. doi: 10.1084/jem.20100643 [published Online First: 2010/09/08]
20. Tan J, Yu Z, Huang J, et al. Increased PD-1+Tim-3+ exhausted T cells in bone marrow may influence the clinical outcome of patients with AML. *Biomark Res* 2020;8:6. doi: 10.1186/s40364-020-0185-8

21. Gorman JV, Starbeck-Miller G, Pham NL, et al. Tim-3 directly enhances CD8 T cell responses to acute Listeria monocytogenes infection. *J Immunol* 2014;192(7):3133-42. doi: 10.4049/jimmunol.1302290
22. Azizi E, Carr AJ, Plitas G, et al. Single-Cell Map of Diverse Immune Phenotypes in the Breast Tumor Microenvironment. *Cell* 2018;174(5):1293-308 e36. doi: 10.1016/j.cell.2018.05.060
23. Taylor GS, Long HM, Brooks JM, et al. The immunology of Epstein-Barr virus-induced disease. *Annu Rev Immunol* 2015;33:787-821. doi: 10.1146/annurev-immunol-032414-112326
24. Schmied S, Gostick E, Price DA, et al. Analysis of the functional WT1-specific T-cell repertoire in healthy donors reveals a discrepancy between CD4(+) and CD8(+) memory formation. *Immunology* 2015;145(4):558-69. doi: 10.1111/imm.12472
25. Chapuis AG, Ragnarsson GB, Nguyen HN, et al. Transferred WT1-Reactive CD8+ T Cells Can Mediate Antileukemic Activity and Persist in Post-Transplant Patients. *Sci Transl Med* 2013;5(174):174ra27. doi: 5/174/174ra27 [pii]

10.1126/scitranslmed.3004916 [published Online First: 2013/03/01]
26. Doubrovina E, Carpenter T, Pankov D, et al. Mapping of novel peptides of WT-1 and presenting HLA alleles that induce epitope-specific HLA-restricted T cells with cytotoxic activity against WT-1(+) leukemias. *Blood* 2012;120(8):1633-46. doi: blood-2011-11-394619 [pii]

10.1182/blood-2011-11-394619 [published Online First: 2012/05/25]
27. Sun F, Guo ZS, Gregory AD, et al. Dual but not single PD-1 or TIM-3 blockade enhances oncolytic virotherapy in refractory lung cancer. *J Immunother Cancer* 2020;8(1) doi: 10.1136/jitc-2019-000294
28. Lee J, Su EW, Zhu C, et al. Phosphotyrosine-dependent coupling of Tim-3 to T-cell receptor signaling pathways. *Mol Cell Biol* 2011;31(19):3963-74. doi: 10.1128/MCB.05297-11
29. Das M, Zhu C, Kuchroo VK. Tim-3 and its role in regulating anti-tumor immunity. *Immunol Rev* 2017;276(1):97-111. doi: 10.1111/imr.12520
30. Ahn E, Araki K, Hashimoto M, et al. Role of PD-1 during effector CD8 T cell differentiation. *Proc Natl Acad Sci U S A* 2018;115(18):4749-54. doi: 10.1073/pnas.1718217115
31. Odorizzi PM, Pauken KE, Paley MA, et al. Genetic absence of PD-1 promotes accumulation of terminally differentiated exhausted CD8+ T cells. *J Exp Med* 2015;212(7):1125-37. doi: 10.1084/jem.20142237
32. Friese C, Harbst K, Borch TH, et al. CTLA-4 blockade boosts the expansion of tumor-reactive CD8(+) tumor-infiltrating lymphocytes in ovarian cancer. *Sci Rep* 2020;10(1):3914. doi: 10.1038/s41598-020-60738-4
33. Rudqvist NP, Pilones KA, Lhuillier C, et al. Radiotherapy and CTLA-4 Blockade Shape the TCR Repertoire of Tumor-Infiltrating T Cells. *Cancer Immunol Res* 2018;6(2):139-50. doi: 10.1158/2326-6066.CIR-17-0134
34. Han J, Duan J, Bai H, et al. TCR Repertoire Diversity of Peripheral PD-1(+)CD8(+) T Cells Predicts Clinical Outcomes after Immunotherapy in Patients with Non-Small Cell Lung Cancer. *Cancer Immunol Res* 2020;8(1):146-54. doi: 10.1158/2326-6066.CIR-19-0398

Figures

Figure 1

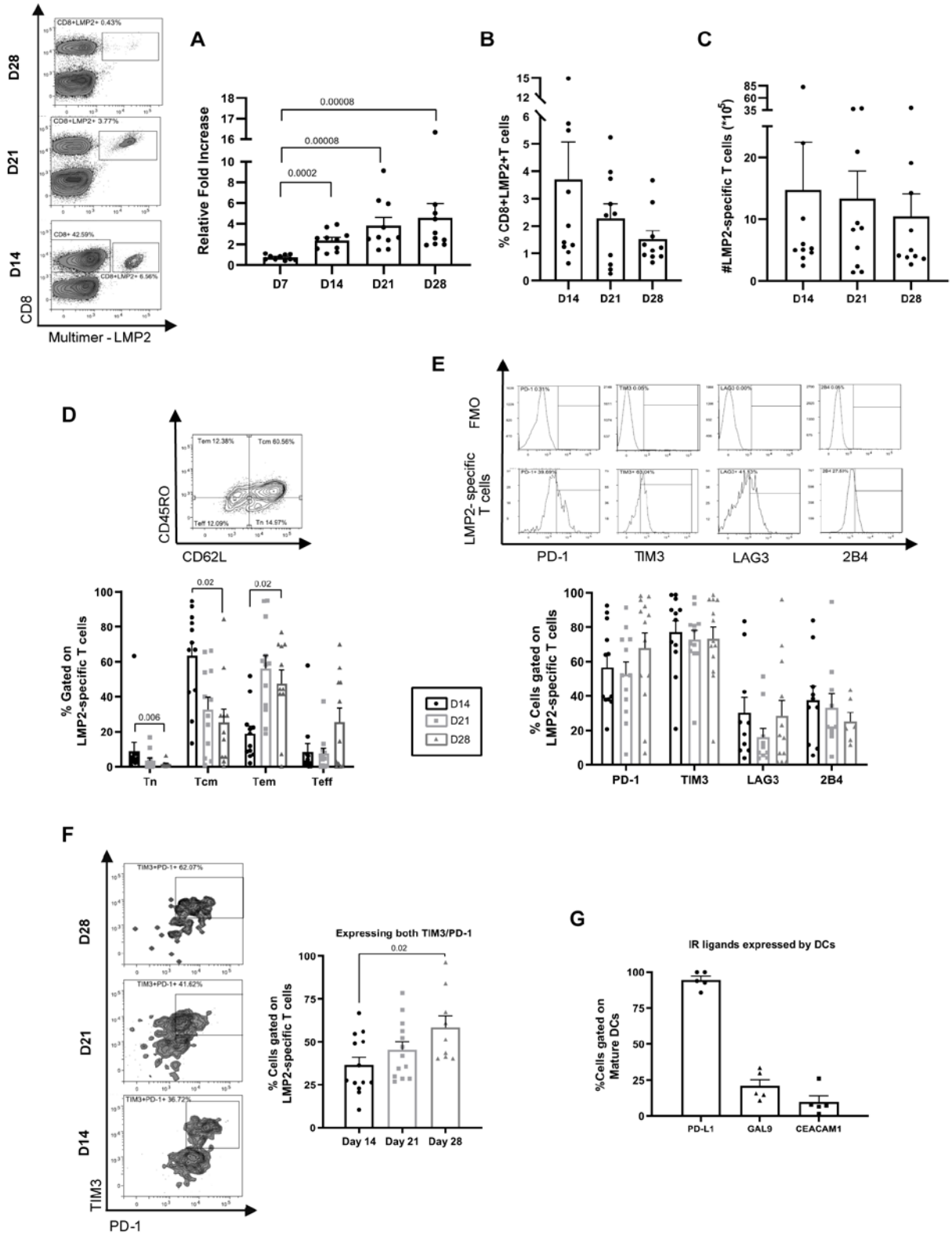

Figure 1. Repeated antigenic encounters ex vivo leads to antigen-specific T-cell exhaustion. (A) Representative fluorescent multimer staining of $LMP2_{426-434}$-specific $CD8^+$ T cells (LMP2) and total cellular expansion (expressed as fold change relative to culture input – $15x10^6$ cells). (B) Percentages, as well as (C) calculated number of antigen-specific T cells at the indicated time points (n=10 different donors). (D) Representative staining to determine naïve (Tn), central memory (Tcm), effector memory (Tem), and effector T cells (Teff) and the percentage of HLA-A02/$LMP2_{426-434}$ multimer positive $CD8^+$ T cells within these categories at different culture time points (n= 12 different donors). (E) Representative histograms of immune checkpoint expression evaluated relative to fluorescence minus one (FMO) control in HLA-A0201-$LMP2_{426-434}$ (LMP2) multimer-stained T cells and compiled results from 12 different donors. (F) Representative staining of PD-1 and TIM-3 co-expression and compiled results from 9-13 different donors. (H) Percentage expression of PD-1 and TIM-3 ligands on dendritic cells used to stimulate T cells (n=5 different donors). Significant p values are indicated on figure panels. All error bars represent standard deviation to the mean (SEM).

Figure 2

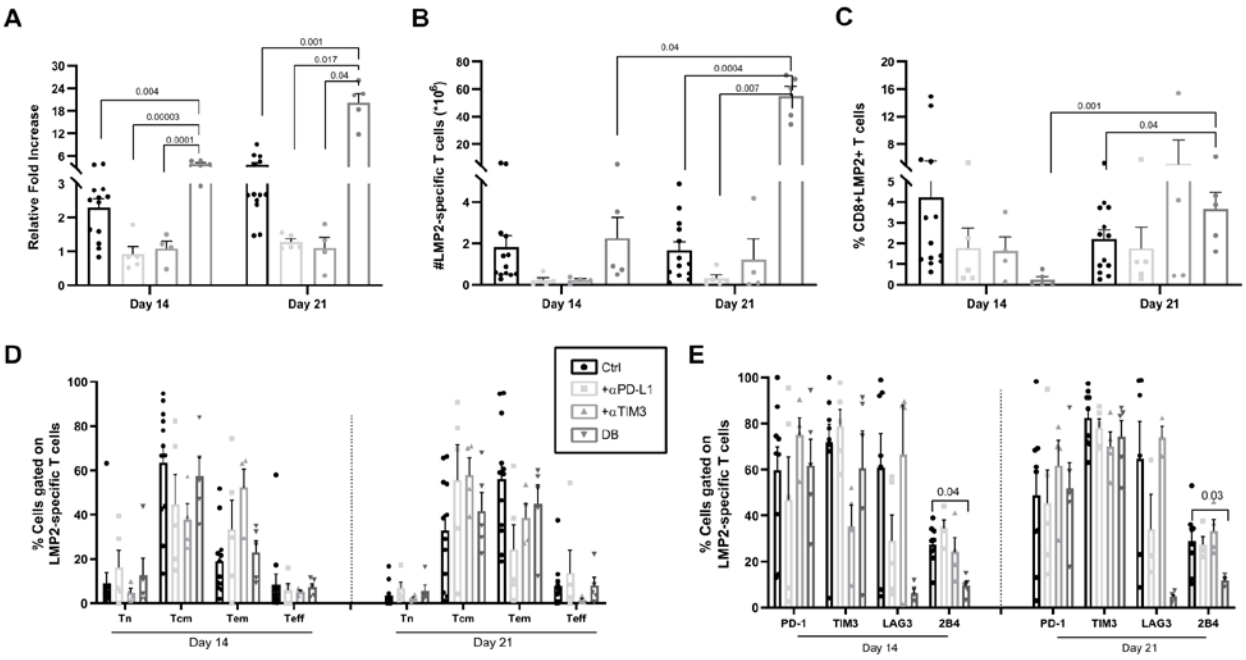

Figure 2. Dual but not single PD-L1 and TIM-3 blockade improves T-cell expansion. (A) Total cell expansion relative to input at the beginning of the culture in function of time and culture condition; no blocking antibodies (ctrl), anti-PD-L1 (α-PD-L1), anti-TIM3 (α-TIM3) or both (double blockade - DB). Absolute count (B) and percentage (C) of HLA-A0201-LMP2$_{426-434}$ (LMP2) multimer positive T cells in the same conditions and at the same time-points. (D) T-cell differentiation phenotypes; naïve (Tn), central memory (Tcm), effector memory (Tem) and effector T cells (Teff) and (E) percentages of LMP2 multimer positive T cells expressing immune checkpoints in the function of culture conditions and time-points (n=4-10 different donors). Significant (<0.05) p-values are indicated on the figure panels. All error bars represent SEM.

Figure 3

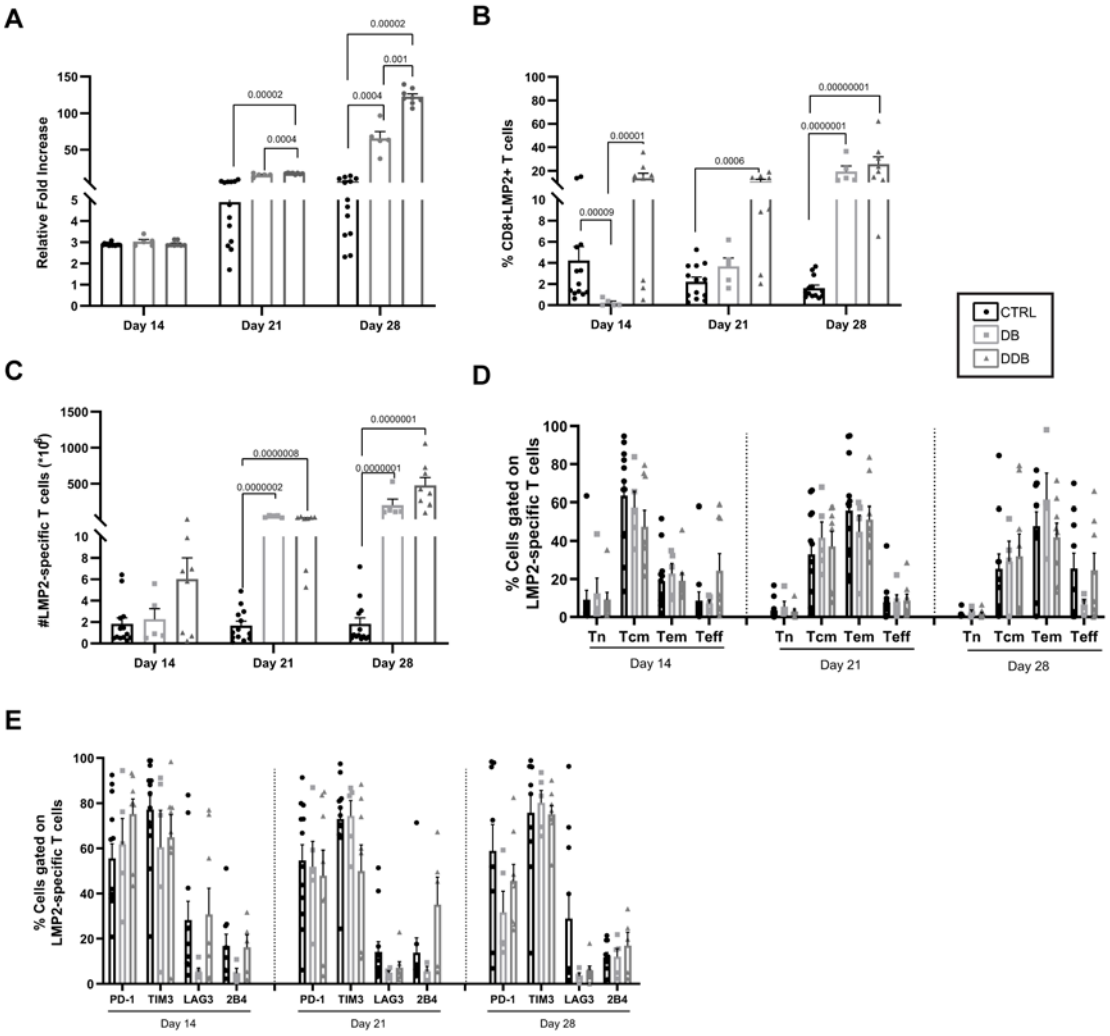

Figure 3. Delayed double blockade (DDB) further improves T-cell yield. (A) Total T-cell expansion relative to input at day 0 in the function of time and culture condition; no blocking antibodies (Ctrl), double anti-PD-L1 and anti-TIM-3 applied at culture initiation (double blockade – DB), anti-PD-L1 introduced at day 0 and anti-TIM-3 introduced at day 7 (delayed double blockade – DDB). (B) Percentages and (C) absolute counts of HLA-A0201-LMP2$_{426-434}$ (LMP2) multimer positive T cells from the same cultures. (D) T-cell differentiation phenotypes and (E) immune checkpoint expression of LMP2 multimer positive cells in the same culture conditions and time-points (n=8 different donors). Significant (<0.05) p-values are indicated on the figure panels. All error bars represent SEM.

Figure 4

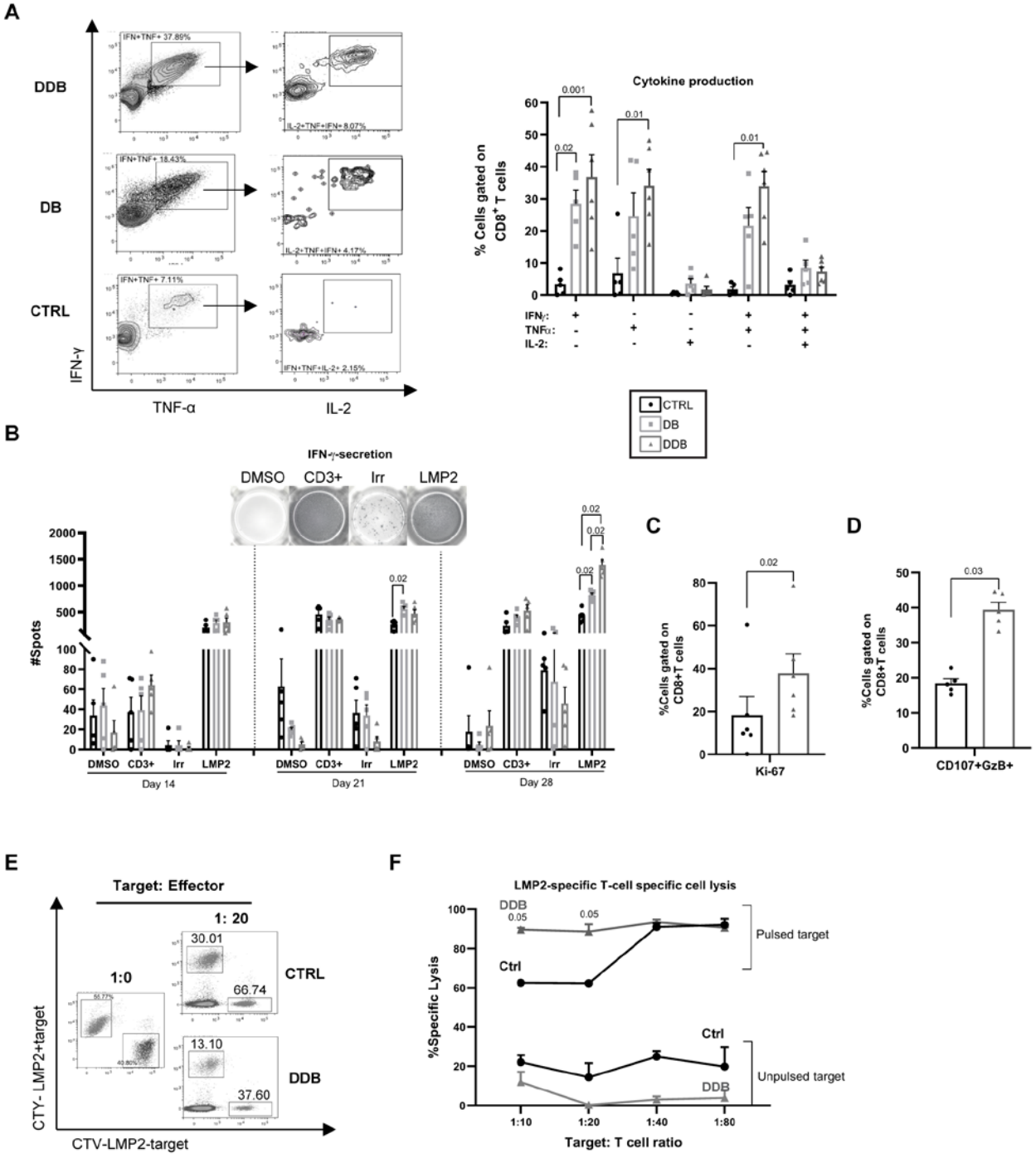

Figure 4. DDB expands a high proportion and number of functional antigen-specific T cells. (A) Representative dot plots showing intracellular cytokine secretion following $LMP2_{426-434}$ antigenic re-stimulation at day 28 and compiled results from 6 independent donor cultures; expansion with no blocking antibodies (CTRL), anti-PD-L1 and anti-TIM3 antibodies both introduced at the beginning of the culture

(DB) or both antibodies but anti-TIM3 introduced at day 7 (DDB). (B) IFN-γ ELISpot results using 50,000 cells per condition harvested from the cultures at the indicated time-points and using the following stimulating conditions: vehicle only (DMSO), anti-CD3 (CD3, positive control), irrelevant peptide (Irr.), $LMP2_{426-434}$ peptide (LMP2). (C) Percentage of Ki-67 staining at day 28 among $CD8^+$ T cells from the ctrl vs DDB cultures (n=5 different donors) and (D) co-expression of surface CD107a and intracellular granzyme-b (GzB) as surrogate for degranulation following $LMP2_{426-434}$ exposure. (E) Fluorescence-based cytotoxicity assay (cell tracer yellow – CTY or cell tracer violet – CTV) showing loss of targets loaded (LMP2+) or not (LMP2-) with the $LMP2_{426-434}$ antigen (numbers indicate percentages of total events) and (F) compiled results at different target:T-cell ratio (from 3 different donors). The significant p-values are indicated on the panels and error bars indicate SEM.

Figure 5

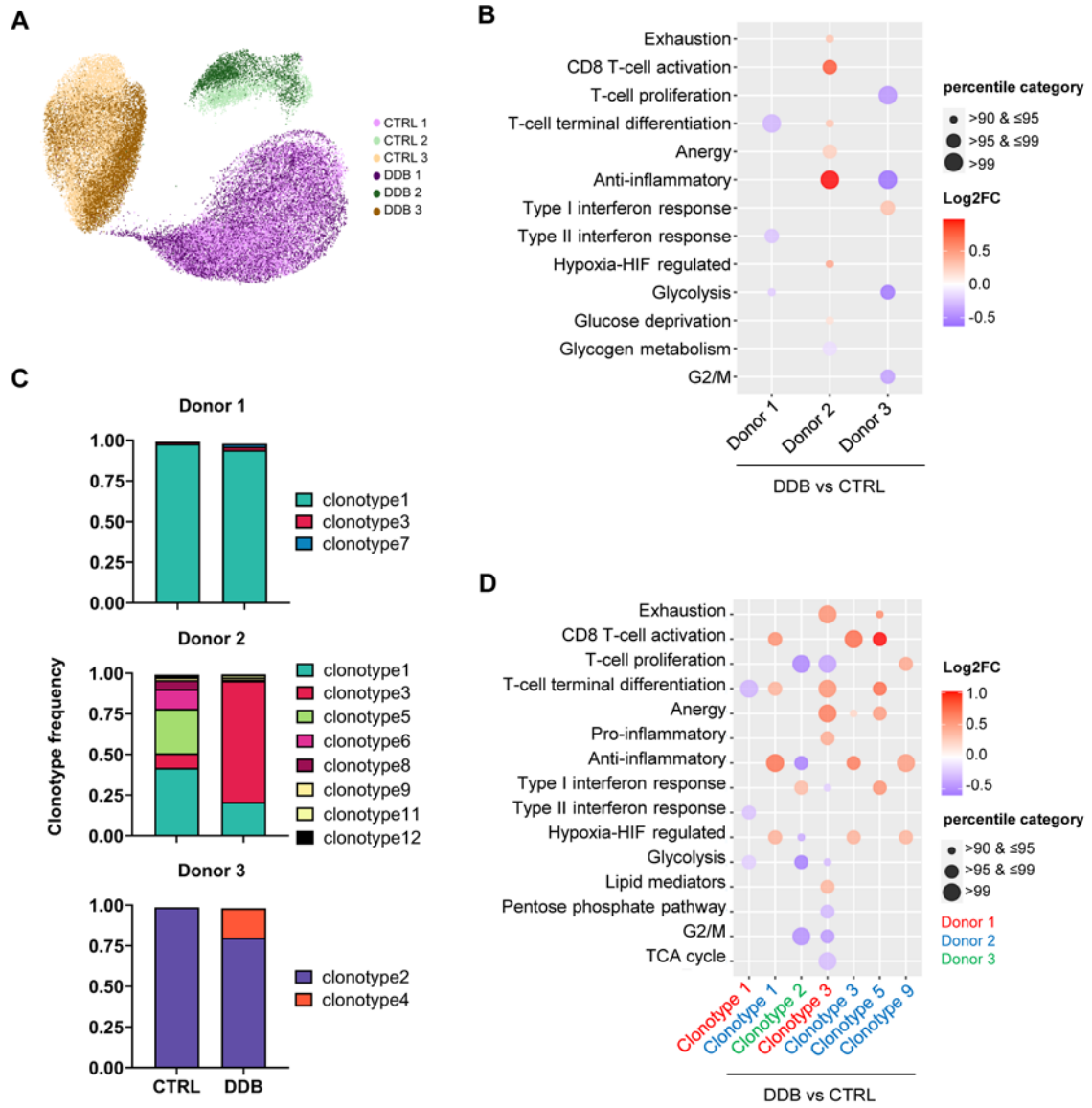

Figure 5. Single-cell RNA-sequencing of antigen-specific T cells after double immune checkpoint inhibition.

(A) T-stochastic neighbor embedding (t-SNE) of normalized single-cell gene expression after dimensionality reduction from control (CTRL) and delayed double blockade (DDB) conditions, color coded by donor and experimental condition (CTRL, DDB). (B) Dot plot representing the change in the expression of genes related to pathways of interest in the DDB condition compared to the CTRL condition. The color of the dots represents the log2 fold-change of the genes in the pathway and the size of the dot is representative of the

667 percentile ranking of the comparison in random gene sets (see Methods). (C) Clonotype frequencies in the
668 CTRL and DDB conditions for each donor. (D) Similar to (B) comparing the cells of selected
669 clonotypes/patients between the two experimental conditions. The donor of origin is color coded.

670

671

Figure 6

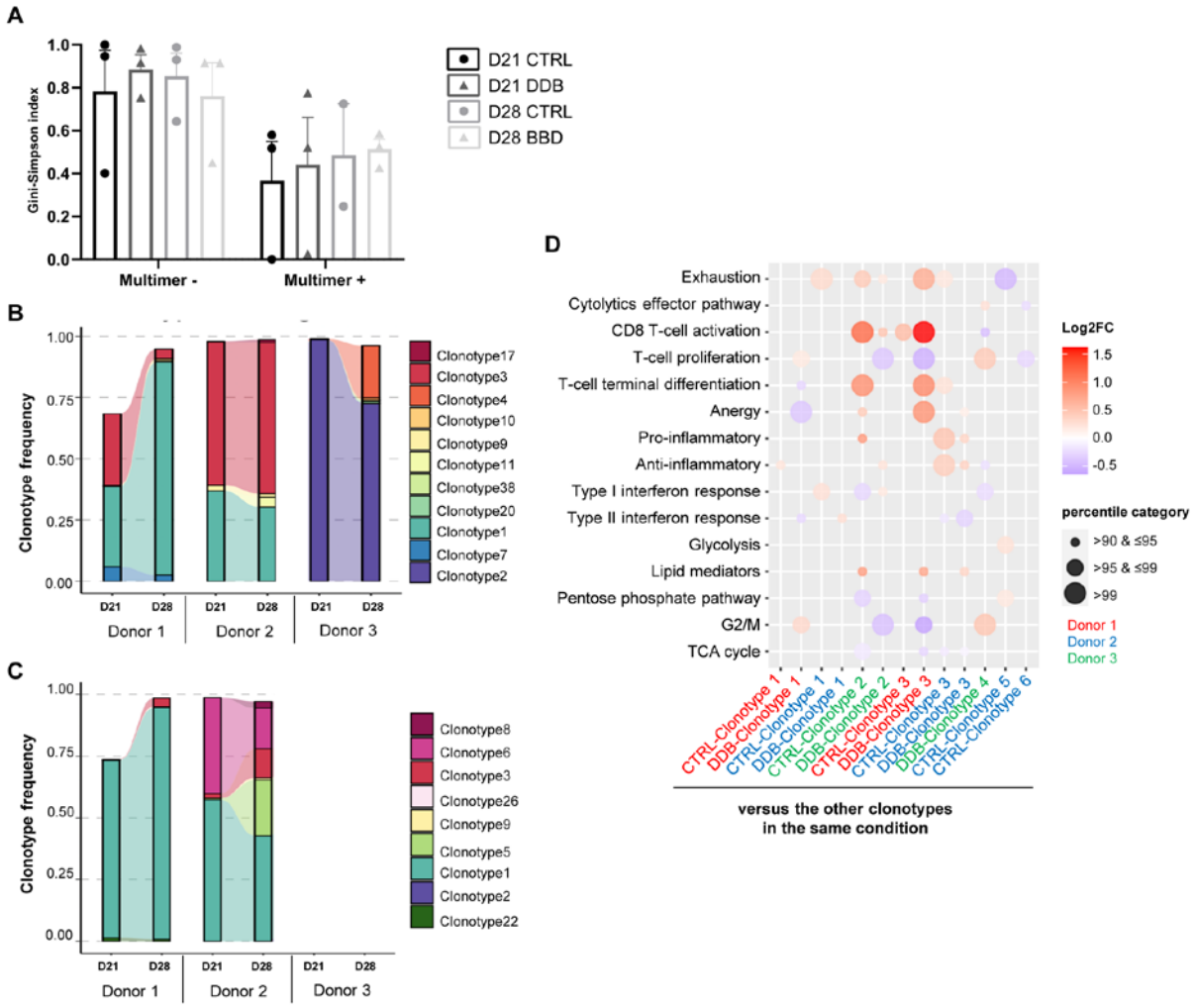

Figure 6. Impact of DDB on clonal diversity and stability in time.

(A) Estimate of TCR repertoire diversity using the Gini-Simpson index among HLA-multimer negative and positive T cells at day 21 and 28. (B) Clonal hierarchy and clonal relatedness among HLA-A0201-LMP2$_{426-434}$ multimer positive T cells between day 21 and 28 based on the day 28 repertoire in the DDB (B) or control condition (C) based on bulk CDR3 sequencing. The control condition in Donor 3 was not assessed due poor RNA quality at day 28. (D) Dot plot representing the change in the expression of genes related to pathways of interest when comparing a clonotype of interest in a donor/experimental condition to all the other clonotypes in the same donor/condition. The clonotypes selected are those whose abundance vary by more than 20% between day 21 and 28.

Figure 7

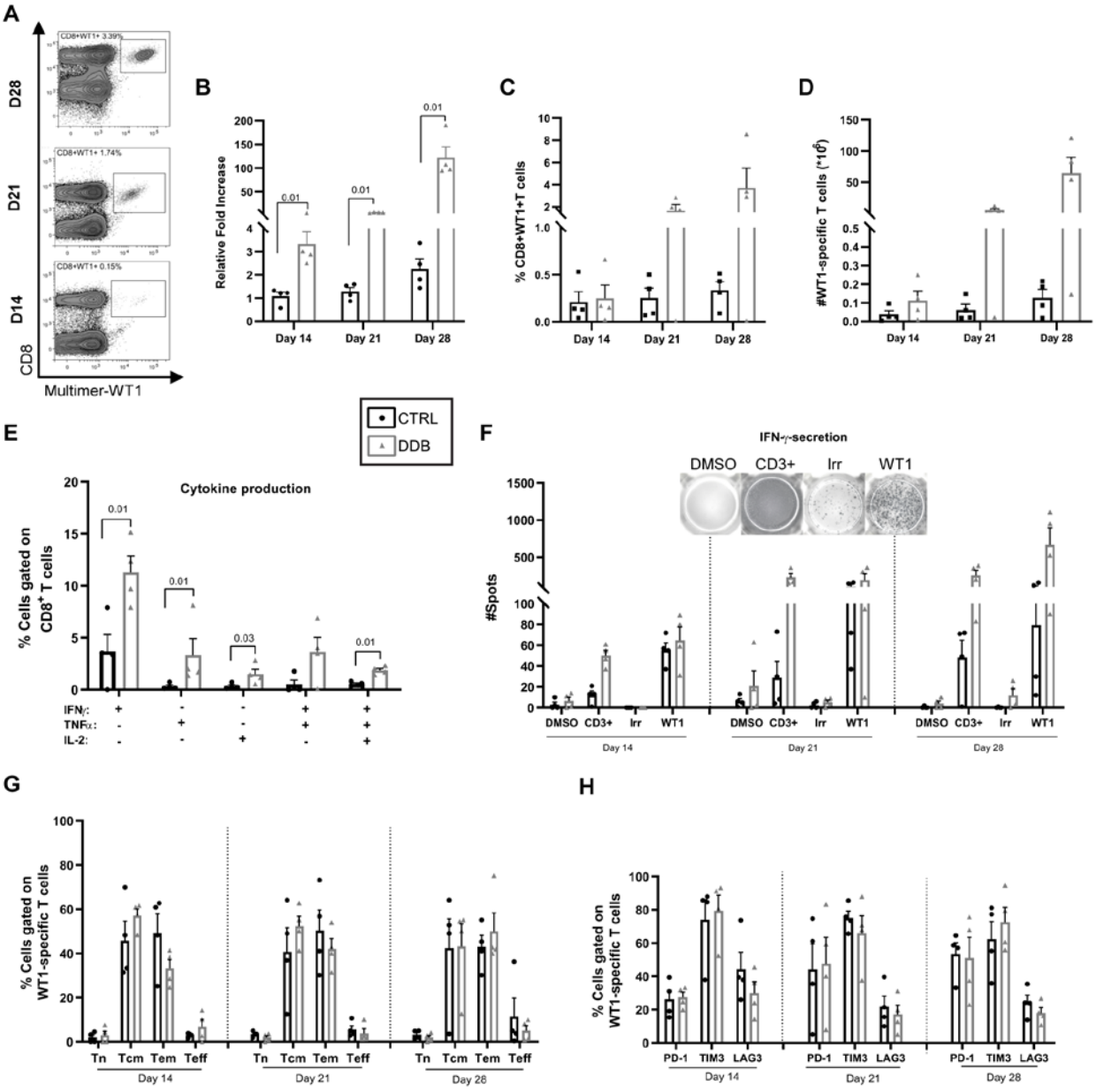

Figure 7. Improved expansion of functional WT1-specific T cells with DDB. (A) Representative HLA-A0201-WT1$_{37-45}$ multimer staining (WT1) of CD8$^+$ T cells. (B) Cell expansion expressed as fold increase relative to cell input at the beginning of the culture (15x10^6) in ctrl (no blocking antibodies) or delayed double anti-PD-L1 and anti-TIM3 blockade (DDB) condition, as well as percentage (C) and absolute numbers (D) of WT1-specific T cells at different time-points in culture. (E) Proportion of intracellular cytokine expression following WT1 exposure at day 28 of the culture in CD8$^+$ cells and (F) IFN-γ ELISpot results at days 14, 21, and 28 of culture following exposure to vehicle alone (DMSO), a peptide not used in the culture (irrelevant,

691 Irr) as negative controls, anti-CD3ε (positive control) and the targeted peptide (WT1). (G) T-cell
692 differentiation; naïve (Tn), central memory (Tcm), effector memory (Tem), and effector T cells (Teff) and
693 (H) percentage of immune checkpoint surface expression on WT-1 specific T cells. Four (4) different
694 donors, p-values are indicated on the figures, error bars indicate SEM.
695